

---

O.YA. OLIKH

Taras Shevchenko National University of Kyiv, Faculty of Physics  
(64, Volodymyrs'ka Str., Kyiv 01601, Ukraine; e-mail: olikh@univ.kiev.ua)

## FEATURES OF CHARGE TRANSPORT IN Mo/*n*-Si STRUCTURES WITH A SCHOTTKY BARRIER

---

PACS 73.40.Sx

*Forward and reverse current-voltage characteristics of Mo/*n*-Si Schottky barrier structures have been studied experimentally in the temperature range 130 ÷ 330 K. The Schottky barrier height is found to increase and the ideality factor to decrease, as the temperature grows. The obtained results are analyzed in the framework of a non-uniform contact model. The average value and the standard deviation of a Schottky barrier height are determined to be 0.872 and 0.099 V, respectively, at  $T = 130 \div 220$  K and 0.656 and 0.036 V, respectively, at  $T = 230 \div 330$  K. Thermionic emission over the non-uniform barrier and tunneling are shown to be the dominant processes of charge transfer at a reverse bias voltage.*

*Keywords:* inhomogeneous Schottky barrier, thermionic emission, silicon

### 1. Introduction

Structures with a Schottky contact are widely used, while manufacturing high-speed logic, integrated, and opto-electronic elements. Therefore, the interest of scientists to similar structures is quite obvious. One of the basic approaches to the description of a current through the metal–semiconductor (MS) contact is the theory of thermionic emission (TE). In an ideal case, the TE current  $I$  through the structure is described by the expression [1–3]

$$I = I_S \{ \exp[qV/(kT)] - 1 \}, \quad (1)$$

where  $V$  is the bias voltage applied to the structure,

$$I_S = SA^*T^2 \exp[-q\Phi_b/(kT)] \quad (2)$$

is the saturation current at the reverse bias,  $S$  is the contact area,  $A^*$  is the effective Richardson constant, and  $\Phi_b$  is the Schottky barrier height (SBH). The latter is defined as the difference between metal's work function and the semiconductor electron affinity [1]. However, expression (1) is too simplified for the case of real MS structures, for which such phenomena as

the action of image forces, the presence of an intermediate dielectric layer and electron states at the interface, a non-uniformity of contact, and a drop of the applied voltage not only across the depletion region in the semiconductor have to be taken into account. As a consequence, the following equation is often used to describe the TE current through the Schottky contact [3]:

$$I = I_S \exp\left[\frac{q(V - IR_S)}{nkT}\right] \left\{ 1 - \exp\left[-\frac{q(V - IR_S)}{kT}\right] \right\}, \quad (3)$$

where  $n$  is the ideality factor,  $R_S$  is the series resistance, and  $I_S$  is also described by expression (2), but the quantity  $\Phi_b$ , as well as  $n$ , becomes dependent on the contact state and the temperature  $T$ . Besides TE, probable mechanisms of charge transfer in MS structures are generation-recombination processes in the contact region, various current leakage processes, tunneling, thermally induced field emission (local energy levels can play a considerable role in the last two cases), and so forth [3–10]. As a result, the total current is often considered as a sum of several terms. Each of them is associated with a specific charge transfer mechanism, which can domi-

nate in that or another temperature or field range [4–6]. In particular, in many cases—such as generation-recombination currents, thermally induced field emission, trap-assisted tunneling, and so on—those terms look similar to those in Eq. (3). However, while describing the saturation current, other expressions, different from Eq. (2), have to be applied.

Note that, owing to a wide variety of affecting factors, the problem of predicting a specific charge transfer mechanism in structures with a Schottky barrier under definite conditions, including temperature ones, is a complicated task, which has no general solution. On the other hand, the technology development assumes that the scope of requirements should be extended to include the conditions, under which semiconductor devices would operate. Therefore, the aim of this work was to elucidate the mechanisms of charge transfer at forward and reverse biases in Mo/n-Si structures, which were fabricated following the standard industrial technology, at temperatures below their nominal operating range. Analogous structures are used at manufacturing the rectifying diodes, in particular, of 2D219 type. As a result, the measurement of current-voltage characteristics (CVCs) was selected as the main method of researches. The data obtained are analyzed in the framework of the inhomogeneous barrier model [11–13]. Lately, this model has been used more and more widely for the interpretation of experimental data obtained for various structures with a Schottky barrier different by their composition [14–20].

## 2. Specimen Fabrication. Measurement and Calculation Techniques

In our researches, we used Schottky diodes with the following structure. An epitaxial  $n$ -Si:P layer  $0.2 \mu\text{m}$  in thickness was deposited on a  $n^+$ -Si:Sb substrate (KES 0.01, a thickness of  $250 \mu\text{m}$ ). A Schottky contact  $2 \text{ mm}$  in diameter was created on the epitaxial layer surface by depositing a molybdenum layer. The other, ohmic, contact was created on the opposite substrate side. The structures were fabricated at the Tomilino Electronic Factory (Russia).

The current-voltage characteristics of the structures concerned were measured in the interval of dc current variation of  $10^{-9}$ – $10^{-2} \text{ A}$  at the forward and reverse biases with a voltage increment of  $0.01 \text{ V}$  and in the temperature interval  $130$ – $330 \text{ K}$ . The spec-

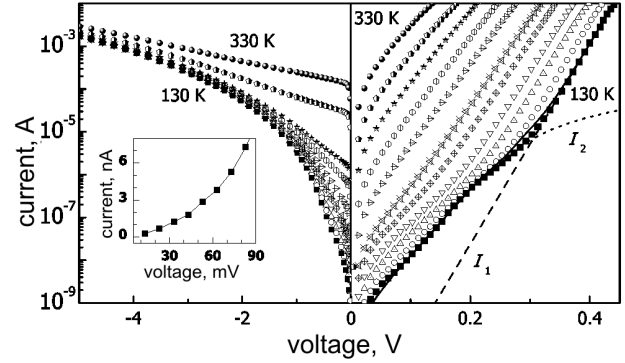


**Fig. 1.** Forward (right panel) and reverse (left panel) CVC branches for Mo/n-Si Schottky diodes measured in the temperature range  $130$ – $330 \text{ K}$  with an increment of  $20 \text{ K}$ . The curves in the right panel illustrate the approximation of the forward CVC branch at  $T = 130 \text{ K}$  by formula (4): current  $I_1$  (dashed curve), current  $I_2$  (dotted curve), and their sum (solid curve); the corresponding approximation parameters are  $n_1 = 1.67$ ,  $n_2 = 2.53$ ,  $I_{S1} = 5.0 \times 10^{-13} \text{ A}$ ,  $I_{S2} = 3.8 \times 10^{-10} \text{ A}$ , and  $R_S = 4.1 \times 10^3 \Omega$ . The initial section of the forward CVC branch at  $T = 130 \text{ K}$  is shown in the inset

imen temperature was monitored with the use of a copper-constantan thermocouple.

Some examples of forward and reverse CVC branches registered at various temperatures are depicted in Fig. 1. One can see that, at temperatures higher than  $250 \text{ K}$ , the forward CVC branches are almost linear on the semilogarithmic scale, within the interval of current variation being of about three orders of magnitude. At the same time, at  $T < 210 \text{ K}$ , the total current can be divided into two components. In particular, for the CVC associated with the current that dominates at low biases, the influence of the series resistance is substantial, which is evidenced by a deviation of the exhibited curves from linearity in the interval  $7 \times 10^{-8} \text{ A} < I < 5 \times 10^{-7} \text{ A}$ . In this connection and taking Eq. (3) into account, the following expression was used to describe the forward CVC branches:

$$I = I_1 + I_2 = I_{S1} \exp\left(\frac{qV}{n_1 kT}\right) \left[1 - \exp\left(-\frac{qV}{kT}\right)\right] + I_{S2} \exp\left[\frac{q(V - IR_S)}{n_2 kT}\right] \left\{1 - \exp\left[-\frac{q(V - IR_S)}{kT}\right]\right\}. \quad (4)$$

Here, the first term prevails at  $I > 10^{-5} \text{ A}$ , and the second one at  $I < 5 \times 10^{-7} \text{ A}$ . Note that another

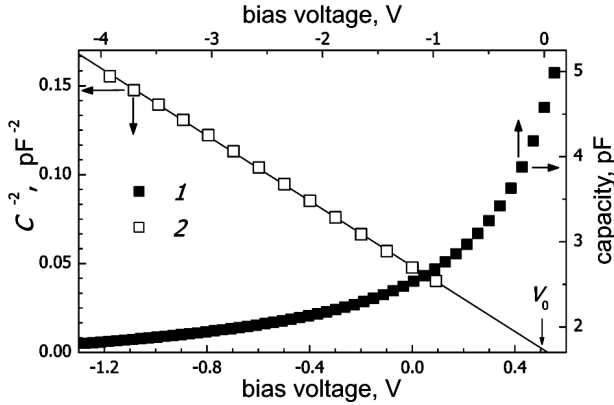


**Fig. 2.** Dependence of the capacity  $C$  (curve 1) and the quantity  $C^{-2}$  (curve 2) on the applied voltage for Mo/*n*-Si Schottky diodes at  $T = 295$  K. Points correspond to experimental data, and the curve to their linear approximation

known technique used to make allowance for the existence of CVC peculiarities at low biases consists in the insertion of a shunting resistance rather than the term  $I_2$ . However, in our opinion, such an approach is not justified in this case, because the forward CVC branch is not linear even at the lowest biases (see the inset in Fig. 1).

In order to determine the fitting parameters, the following procedure was used. Two sections were selected in the forward CVC branch, in which  $10^{-5}$  A  $< I < 10^{-2}$  A and  $10^{-9}$  A  $< I < 10^{-7}$  A, respectively. The data for the former were used to plot the dependence of the quantity  $\ln I/[1 - \exp(-qV/kT)]$  on  $V$ . The obtained curve was approximated by a straight line, the slope and the free term of which were related to the magnitudes of  $n_1$  and  $I_{S1}$ , respectively. From the data for the latter section and using the Cheung [21] and Gromov [22] methods, the magnitude of  $R_S$  was determined. The application of two techniques was aimed at enhancing the reliability of data obtained. The corresponding values turned out to be equal to each other to within 10%. After the value for  $R_S$  had been determined, the quantity  $V$  in the latter section was replaced by the effective voltage  $V^* = V - IR_S$ . Then the  $I_{S2}$ - and  $n_2$ -values were determined following the procedure described above.

Figure 1 illustrates an example of the approximation of the experimental forward CVC branch registered at a certain temperature. The approximation was carried out with the use of formula (4), and the parameters were obtained following the described

routine. A good coincidence between the calculated curve and the experimental points is evident.

Basing on expression (2) and obtained  $I_{S1}$ - and  $I_{S2}$ -values, we also determined the corresponding SBHs at the zero bias,  $\Phi_{b1}$  and  $\Phi_{b2}$ , respectively. In the calculations, we assumed that, for *n*-Si,  $A^* = 112$  A/cm<sup>2</sup>/K<sup>2</sup> [23] and  $S = 3.14 \times 10^{-6}$  m<sup>2</sup>.

For monitoring the doping level, we measured the capacity-voltage (volt-farad) characteristics (VFCs) of the studied structures at room temperature,  $T = 295$  K; see Fig. 2. The results obtained show that the concentration of charge carriers in the epitaxial layer is  $N_D = 1.3 \times 10^{23}$  m<sup>-3</sup>. In addition, with the help of the expression [3, 23]

$$\Phi_{b,CV} = V_n + V_0 + kT/q, \quad (5)$$

we determined the SBH  $\Phi_{b,CV} = (0.689 \pm 0.002)$  V. In Eq. (5), the quantity  $qV_n = kT \ln(N_C/N_D)$  equals the energy difference between the conduction band bottom and the Fermi level position,  $N_C$  is the effective density of states near the conduction band bottom, and  $V_0$  is the abscissa of intersection point between the voltage axis and a straight line approximating the dependence of  $C^{-2}$ , where  $C$  is the capacity of a Schottky diode, on the reverse bias voltage. Note that the SBH determined in such a way should exceed the corresponding value obtained with the use of CVCs [3].

### 3. Results and Their Discussion

First, let us consider the features in the current that prevails at high temperatures and high biases; it is  $I_1$ . The obtained temperature dependences of parameters are shown in Fig. 3. One can see that, the value of  $\Phi_{b1}$  increases, as the temperature grows. It was experimentally demonstrated [24, 25] that the opposite tendency has to be observed at the temperature elevation in real structures with a uniform Schottky barrier, provided that the TE dominates, with the temperature coefficients for the reduction of the SBH and the energy gap width  $E_G$  being very close to each other in this case. On the other hand, it is known that the SBH determined with the help of CVCs can differ from the real one. In particular, the authors of work [26] assert the necessity of carrying out measurements at a constant current across the contact and propose to use the expression

$$\Phi_{\text{bef}} = n_{I_C} \Phi_b - (n_{I_C} - 1)(kT/q) \ln(SA^*T^2/I_C), \quad (6)$$

where  $n_{I_C}$  is the ideality factor at a definite constant current  $I_C$ , for the evaluation of the effective barrier height  $\Phi_{\text{bef}}$ . In the cited work [26], it was shown that, in the case of TE through a homogeneous contact, the magnitude of  $\Phi_{\text{bef}}$  almost coincides with the real barrier height and the both quantities have the same temperature dependence.

We calculated  $\Phi_{\text{bef}}$  according to formula (6) at  $I_C = 10^{-3}$  A (Fig. 3, curve 3). For the sake of comparison, the same figure exhibits the temperature dependence of  $E_G$ . When calculating the latter, we took  $E_G(T) = E_G(0) - \gamma T^2/(T + \beta)$ , where  $E_G(0) = 1.17$  eV,  $\beta = 636$  K, and  $\gamma = 4.73 \times 10^{-4}$  eV/K<sup>2</sup> [27]. One can see that, although the magnitude of  $\Phi_{\text{bef}}$  varies within a much narrower interval, its temperature dependence also differs from the behavior of  $E_G$ , especially at low temperatures.

On the other hand, there exists a procedure to calculate the parameter  $A^*$  [3, 23] consisting in the plotting of the Richardson dependence, i.e. the dependences of the quantity  $\ln(I_S/T^2)$  on  $(kT)^{-1}$  (see Fig. 4, curve 1). According to Eq. (2), it has to be described by the expression

$$\ln(I_S/T^2) = \ln(SA^*) - q\Phi_b/(kT). \quad (7)$$

However, it is evident that the linear dependence is really observed, but only in two intervals rather than in the whole temperature range. The calculations by formula (7) gave rise to  $\Phi_{bR,I} = (0.141 \pm 0.004)$  V and  $A_{R,I}^* = (3.7 \pm 0.8) \times 10^{-10}$  A/cm<sup>2</sup>/K<sup>2</sup> in the interval 130–220 K and to  $\Phi_{bR,II} = (0.599 \pm 0.003)$  V and  $A_{R,II}^* = (30 \pm 10)$  A/cm<sup>2</sup>/K<sup>2</sup> in the interval 230–330 K. It is evident that the values of  $A_{R,II}^*$  and, especially,  $A_{R,I}^*$  differ from the literature data.

As we know from the literature [28], in the case of a substantial deviation from ideality, it is expedient to use the transformed Richardson dependence for the determination of  $A^*$ , in which the quantity  $(nkT)^{-1}$  rather than  $(kT)^{-1}$  is reckoned along the abscissa axis. However, in our case, the transformed Richardson dependence (Fig. 4, curve 2) is also non-linear.

While summarizing the above consideration, it is necessary to recognize that the obtained results cannot be explained in the framework of the theory for TE through a uniform contact. On the other hand, the model of inhomogeneous Schottky barrier has often been used recently to explain the CVCs of real metal–semiconductor structures [11–13]. In particular, according to the model proposed in work [11], if

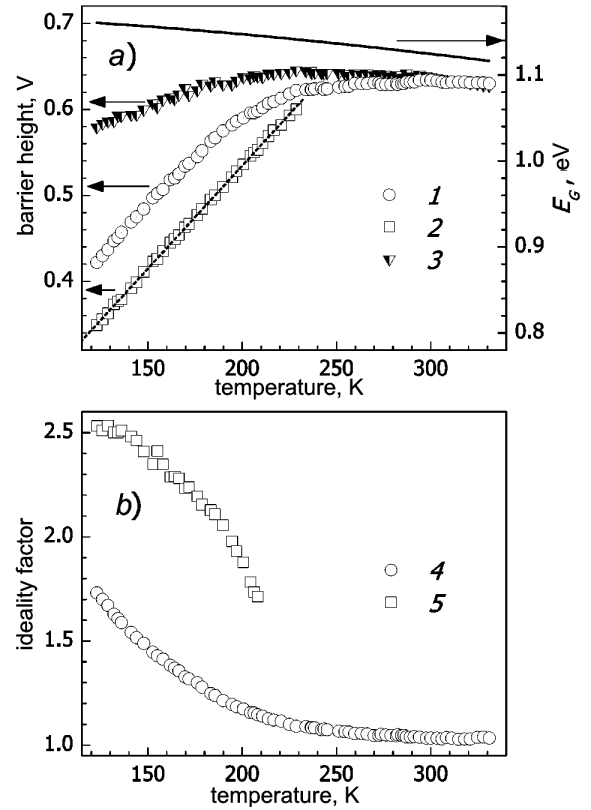


**Fig. 3.** Temperature dependences of the barrier height (a) and the ideality factor (b) for Mo/n-Si Schottky diodes:  $\Phi_{b1}$  (1),  $\Phi_{b2}$  (2),  $\Phi_{\text{bef}}$  (3),  $n_1$  (4), and  $n_2$  (5). The dotted line depicts the linear approximation of curve 2. The solid curve in panel a corresponds to the temperature dependence of the energy gap width in Si

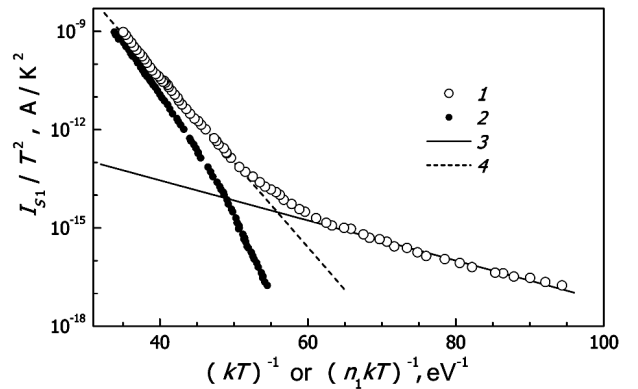


**Fig. 4.** Ordinary (1) and transformed (2) Richardson dependences for  $I_1$ . The straight lines are linear approximations of the data in curve 1 in the intervals  $T = (130 \div 220)$  K (3) and  $T = (230 \div 330)$  K (4)

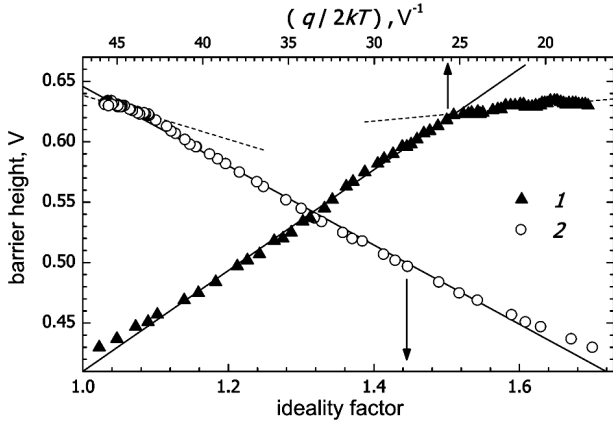


**Fig. 5.** Dependences of  $\Phi_{b1}$ -value on the reciprocal of the doubled temperature (1) and  $n_1$  (2). The straight lines are linear approximations in the intervals  $T = (130 \div 220)$  K (solid lines) and  $T = (230 \div 330)$  K (dotted lines)

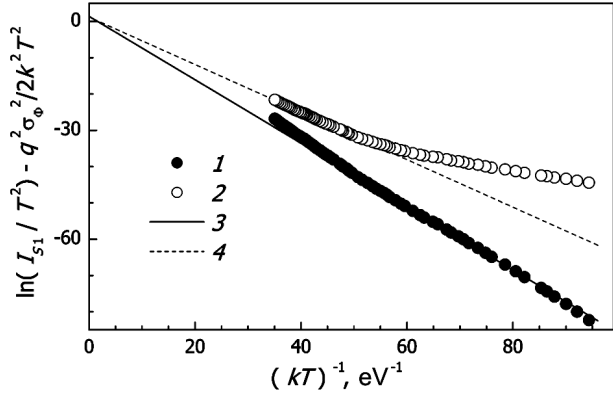


**Fig. 6.** Modified Richardson dependences (10) for  $I_{S1}$ .  $\sigma_0 = 0.099$  (1) and  $0.036$  V (2). Straight lines 3 and 4 are the linear approximations of curve 1 in the interval  $T = (130 \div 220)$  K and curve 2 in the interval  $T = (230 \div 330)$  K, respectively

the SBH is described by a Gaussian distribution, the theory of TE brings about the relation [11, 16–18]

$$\Phi_b = \Phi_b^0 - q\sigma_\Phi^2/(2kT), \quad (8)$$

where  $\Phi_b^0$  is the average SBH, and  $\sigma_\Phi$  is the standard deviation of a barrier height, which characterizes the contact uniformity. The corresponding dependence for our case is depicted in Fig. 5 (curve 1). One can see that the linear dependence really takes place, however, in two separate temperature intervals,  $T = 130 \div 220$  and  $230 \div 330$  K. Linear approximations by formula (8) gave the following fitting parameters:  $\Phi_{bT,I}^0 = (0.872 \pm 0.003)$  V and  $\sigma_{\Phi,I} = (0.099 \pm 0.001)$  V

for the former interval, and  $\Phi_{bT,II}^0 = (0.656 \pm 0.003)$  V and  $\sigma_{\Phi,II} = (0.036 \pm 0.004)$  V for the latter one.

In the framework of another model for the non-uniform Schottky contact [12, 13], the SBH is assumed identical over the whole MS interface, excluding the sections with small areas (patches), where the SBH is lower. The patches may differ from one another by their area and SBH, and the corresponding characteristic parameter is described by the Gaussian distribution [13]. It was shown in a number of works [19, 20] that those theories can be used together. In the case where inhomogeneous patches do exist, relation (8) remains valid, but the quantity  $\Phi_b^0$  means the SBH magnitude in the uniform region.

In the literature [13, 14, 28], the dependence between the  $\Phi_b$ - and  $n$ -values obtained from the CVC analysis was shown to be linear in the case of contacts with local inhomogeneities. Moreover,  $\Phi_b = \Phi_b^0$  at  $n = n_{if}$ , where

$$n_{if} = 1 + \frac{1}{4} \left[ \frac{q^3 N_D}{8\pi^2 \varepsilon_s^3 \varepsilon_0^3 V_{bb}^3} \right]^{1/4} \quad (9)$$

is the ideality factor that takes the influences of image forces into account [14],  $V_{bb} = (\Phi_b^0 - V_n - V)$  is the band bending in the semiconductor layer near the contact,  $\varepsilon_s$  is the semiconductor dielectric constant, and  $\varepsilon_0$  is the dielectric permittivity of vacuum. In the dependence  $\Phi_{b1}(n_1)$ , similarly to the previous cases, two linear sections are observed with a cusp at  $T \approx 225$  K (see Fig. 5, curve 2). The extrapolation procedure gave  $\Phi_{bn,I}^0 = (0.646 \pm 0.005)$  V for the interval  $T = (130 \div 220)$  K and  $\Phi_{bn,II}^0 = (0.64 \pm 0.02)$  V for the interval  $T = (230 \div 330)$  K.

Taking Eqs. (2) and (8) into account, the Richardson dependence for the case of a barrier with different inhomogeneous patches can be written down in a modified form [16, 17]

$$\ln \left( \frac{I_S}{T^2} \right) - \left( \frac{q^2 \sigma_\Phi^2}{2k^2 T^2} \right) = \ln(SA^*) - \frac{q\Phi_b^0}{kT}. \quad (10)$$

The corresponding plots for the obtained  $\sigma_{\Phi,I}$ - and  $\sigma_{\Phi,II}$ -values are shown in Fig. 6. The linear approximations of those curves in the corresponding temperature intervals selected for the determination of  $\sigma_{\Phi,I}$  and  $\sigma_{\Phi,II}$  brought about the following parameters:  $\Phi_{bRM,I}^0 = (0.874 \pm 0.004)$  V and  $A_{RM,I}^* = (125 \pm 20)$  A/cm<sup>2</sup>/K<sup>2</sup> for  $T = (130 \div 220)$  K, and  $\Phi_{bRM,II}^0 = (0.655 \pm 0.003)$  V and  $A_{RM,II}^* = (110 \pm$

Table 1. Determinated parameters for Mo/*n*-Si Schottky diodes

Determination technique	Barrier height, V		Richardson constant, A/cm <sup>2</sup> /K <sup>2</sup>	
	130–220 K	230–330 K	130–220 K	230–330 K
Richardson dependence	0.141	0.599	$3.7 \times 10^{-10}$	32
Dependence $\Phi_b$ versus $n$	0.646	0.64		
Dependence $\Phi_b$ versus $(kT)^{-1}$	0.872	0.656	125	110
Modified Richardson dependence	0.874	0.655		
VFC		0.689	112	
Source[23]				

$\pm 10$ ) A/cm<sup>2</sup>/K<sup>2</sup> for  $T = (230 \div 330)$  K. Note that the magnitudes of  $A_{RM,I}^*$  and  $A_{RM,II}^*$  practically coincide with the corresponding literature data within the measurement errors. The parameters obtained in different ways are listed in Table 1.

The temperature dependence of the ideality factor is known to depend on the charge transfer mechanism. For example, if the thermal field emission (TFE) or deep-level-assisted tunneling dominates, then [3, 7]

$$n = E_{00}/(kT) \coth [E_{00}/(kT)], \quad (11)$$

where  $E_{00}$  is a characteristic energy. Note that, in the TFE case,  $E_{00} = (\hbar/2)[N_D/(m^*\varepsilon_s\varepsilon_0)]^{1/2}$ , where  $m^* = 1.08 \times 9.11 \times 10^{-31}$  kg is the effective electron mass; therefore, for the examined specimens and the temperature interval, there would have been  $n \approx 1$  in this case. However, if TE prevails, the temperature dependence of  $n$  for real contacts is often written down in the form [3]

$$n = 1 + T_0/T, \quad (12)$$

where  $T_0$  is a certain constant. In the case of different patches, it was shown [12, 13, 19] that

$$T_0 = q\sigma_{\Phi}^2/(3kV_{bb}). \quad (13)$$

In Fig. 7, the calculated dependence for the inverse CVC slope,  $nkT$ , and a number of curves calculated by Eqs. (11) and (12) are depicted. One can see that the data obtained for  $n_1$  at high temperatures are described satisfactorily by expression (12) with  $T_0 = 12$  K. On the other hand, the calculations by Eq. (13) and with the use of the obtained  $\Phi_{bT,II}^0$  and  $\sigma_{\Phi,II}$ -values show that, in the temperature interval 230–330 K, the model with local inhomogeneities brings about rather a close value  $T_{0,theory} \approx 11$  K.

Hence, the results presented above testify that the current  $I_1$  can be described in the framework of the model considering TE through a non-uniform barrier. An additional argument in favor of this conclusion is a qualitative coincidence of the conventional and transformed Richardson dependences (Fig. 4) and the temperature dependence of  $n_2$  in the interval 130–220 K (Fig. 7) with the corresponding dependences predicted in the framework of this model (see Fig. 11, *b* in work [13] and Fig. 3 in work [14]). By the way, note that, in the case where the SBH is determined from VFCs, the influence of inhomogeneities is insignificant [17, 29]. Therefore, the  $\Phi_{b,CV}$ -values can be compared with  $\Phi_b^0$ -ones obtained from CVCs.

The only thing that needs a more detailed attention is the difference between the  $\Phi_b^0$ - and  $\sigma_{\Phi}$ -values in different temperature intervals, which is not pre-

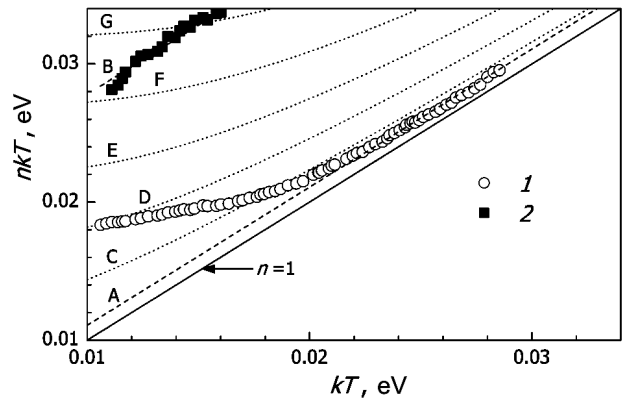
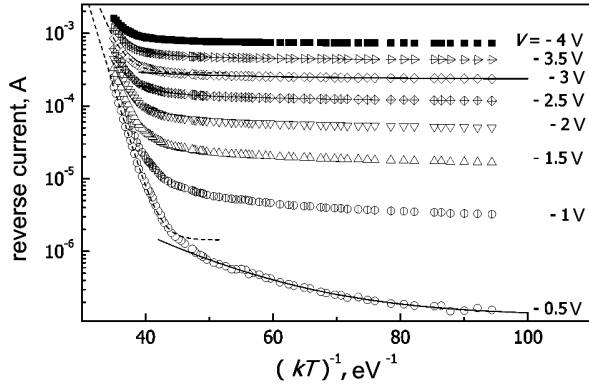
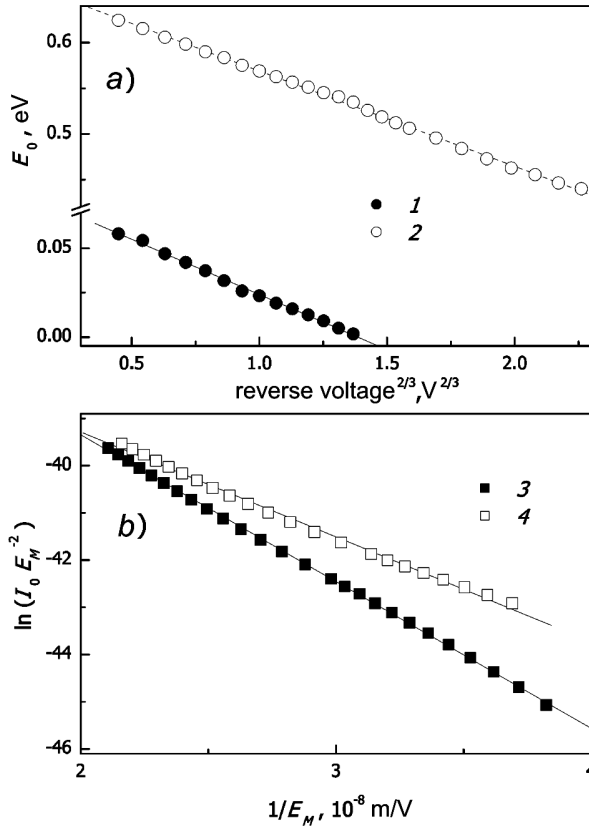


Fig. 7. Temperature dependences of the inverse CVC slope  $n_1$  (1) and  $n_2$  (2). Dotted curves exhibit the results of theoretical calculations according to formulas (12) (curves A and B) and (11) (curves C to G).  $T_0 = 12$  (A) and 206 K (B).  $E_{00} = 12$  (C), 17 (D), 22 (E), 27 (F), and 32 mV (G). Solid straight line corresponds to the ideal case  $n = 1$



**Fig. 8.** Temperature dependences of the reverse current in Mo/*n*-Si Schottky diodes at various bias voltages. Points correspond to the experiment data, lines to their approximations by formula (15) in the intervals  $T = (130 \div 220)$  K (solid lines) and  $T = (230 \div 330)$  K (dotted lines)



**Fig. 9.** Field dependences of the characteristic energy (a) and the temperature-independent component of the reverse current in the Fowler–Nordheim coordinates (b) at  $T = (130 \div 220)$  K (curves 1 and 3) and  $T = (230 \div 330)$  K (curves 2 and 4). Points correspond to experimental data, straight lines to their linear approximations

dicted in the framework of the theory for non-uniform contacts. At the same time, we note that a similar situation has already been observed in practice, e.g., in works [16–18, 30]. Such phenomena were explained as a domination of other, different from TE, mechanisms of charge transfer at low temperatures, such as TFE [16, 18], tunneling [17], and recombination processes [18]. However, in our opinion, the coincidence of the values obtained for  $A_R^*$  with the literature data testifies that it is just the TE theory that is applicable to this case. The changes in the dependence slope in Fig. 5 can be associated with increase in the electron emission rate by defects at the MS interface. Really, the level depletion in some defects at  $T \approx 225$  K should stimulate a reduction of SBH and start a mechanism, owing to which some inhomogeneous patches with elevated concentrations of similar defects cease to be the regions of facilitated current passage due to the effective capture of drifting electrons by traps. As a result,  $\sigma_\Phi$  has to diminish in the high-temperature interval, which is really observed experimentally.

Now, let us come back to the current prevailing at low biases in the low-temperature interval; it is  $I_2$ . In work [13], it was shown that such a current can appear at low temperatures in non-uniform contacts as an additive to  $I_1$  owing to the passage of charge carriers through inhomogeneous regions. The ideality factor for the corresponding CVC section should expectedly and considerably exceed 1 at that, and a substantial influence of the series resistance should also be observed. Just this phenomenon was revealed in our researches (see Figs. 1 and 3). In the case where the current through the patches is governed by the TE mechanism, we have

$$I_S = S f_p A^* T^2 \exp[-q\Phi_{b,p}/(kT)], \quad (14)$$

where  $f_p$  is a multiplier that takes the area of inhomogeneous patches into account, and  $\Phi_{b,p}$  is the average value of SBH in those regions. As is seen from Fig. 3, the SBH  $\Phi_{b2}$ , being calculated on the basis of formula (2), is a linear function of the temperature,  $\Phi_{b2} = a_\Phi + b_\Phi T$ , where  $a_\Phi = (0.056 \pm 0.001)$  V and  $b_\Phi = 2.4 \times 10^{-3}$  V/K. Comparing Eqs. (2) and (14), we may write down that  $f_p = \exp(-qb_\Phi/k) \approx 10^{-12}$  and  $\Phi_{b,p} = a_\Phi = 0.056$  V. As concerns the quantity  $n_2$ , its temperature dependence is also described well by formula (12) with  $T_0 = (206 \pm 5)$  K (Fig. 7).

In Fig. 8, the dependences of the reverse current in examined structures on the reciprocal temperature in the bias interval  $V = -(0.5-4.0)$  V are exhibited. It was found that two temperature sub-intervals, 130–220 and 230–330 K, are also expedient to be considered in this case. In each of them, the temperature dependence of the reverse current at a constant voltage is well approximated by the expression

$$I = CT^2 \exp[-E_0/(kT)] + I_0, \quad (15)$$

where the first term describes the TE current component, and the second one is the temperature-independent one, with the parameters  $C$  and  $E_0$  being also independent of the temperature.

The revealed dependence of the characteristic energy  $E_0$  on the applied voltage evidences the variation of SBH. It is known [3, 13, 31] that a reduction of the barrier height, when the reverse bias is applied, can occur owing to the influence of image forces (in this case, the SBH variation is  $\Delta\Phi_b \sim V^{1/4}$ ) and the electric field ( $\Delta\Phi_b \sim V^{1/2}$ ), as well as to the influence of inhomogeneous regions. In the latter case,  $\Delta\Phi_b \sim V^{2/3}$ , and the proportionality coefficient depends on the local patch parameters [13]. For the structures concerned, the quantity  $E_0$  acquires different values in every temperature interval. However, if the reverse bias increases,  $E_0$  decreases as a linear function of  $V^{2/3}$  in both cases (Fig. 9,a). Hence, the analysis of the reverse CVC branches also confirms that the current through the analyzed structures can be described in the framework of the model for a non-uniform contact with patches, the influence of which on the charge transfer changes at a temperature of about 225 K.

The relative contribution of the temperature-independent component to the reverse current was found to grow with the bias voltage. In Fig. 9,b, the field dependences of the current  $I_0$  are depicted in the Fowler–Nordheim coordinates,  $\ln(I_0/E_M^2)$  versus  $(1/E_M)$ , where  $E_M = [2qN_D V_{bb}/(\epsilon_s \epsilon_0)]^{1/2}$  is the electric field strength at the metal–semiconductor interface [3]. While calculating  $E_M$ , we used the  $\Phi_{bT}^0$ -value obtained for the corresponding temperature interval and the  $V_n$ -value averaged over it. The linear behavior of dependences in Fig. 9,b and the independence of the current component  $I_0$  of the temperature testify to the tunnel origin of this component.

#### 4. Conclusions

In this work, we have experimentally studied the forward and reverse CVC branches for Mo/n-Si structures with a Schottky barrier in the temperature interval 130–330 K. We have found that the barrier height increases with the temperature, whereas the ideality factor demonstrates the opposite tendency. It is shown that the obtained results can be explained in the framework of the model of thermionic emission through a contact containing local regions with lowered values of barrier height. The barrier height in the uniform contact region and the standard deviation of SBH are determined to be 0.872 and 0.099 V, respectively, in the interval 130–220 K, and 0.656 and 0.036 V, respectively, in the interval 230–330 K. For the transformed Richardson dependence, we determined the Richardson constant,  $115 \pm 10$  A/cm<sup>2</sup>/K<sup>2</sup>. The average barrier height in the inhomogeneous regions was determined to be 0.056 V. The reverse current was demonstrated to be driven by both thermionic emission through the non-uniform barrier and tunneling, with the relative contribution of the latter mechanism growing if the bias voltage increases.

*The author is grateful to A.B. Nadochii for his assistance in carrying out VFC measurements.*

1. J.P. Colinge and C.A. Colinge, *Physics of Semiconductor Device* (Kluwer, Dordrecht, 2002).
2. V.I. Strikha, *Contact Phenomena in Semiconductors* (Vyshcha Shkola, Kyiv, 1982) (in Russian).
3. E.H. Rhoderick and R.H. Williams, *Metal Semiconductor Contacts* (Clarendon, Oxford, 1988); S.M. Sze, *Semiconductor Devices: Physics and Technology* (Wiley, New York, 1985).
4. E. Arslan, S. Altindal, S. Ozelcik, and E. Ozbay, *J. Appl. Phys.* **105**, 023705 (2009).
5. D. Donoval, A. Chvala, R. Sramaty, J. Kovac, J.-F. Carlin, N. Grandjean, G. Pozzovivo, J. Kuzmik, D. Pogany, G. Strasser, and P. Kordos, *Appl. Phys. Lett.* **96**, 223501 (2010).
6. S. Huang *et al.*, *Semicond. Sci. Technol.* **24**, 055005 (2009).
7. V.V. Evstropov, Yu.V. Zhilyaev, M. Dzhumaeva, and N. Nazarov, *Fiz. Tekh. Poluprovodn.* **31**, 152 (1997).
8. C.H. Lee and K.S. Lim, *Appl. Phys. Lett.* **75**, 569 (1999).
9. D.M. Sathaiyaa and S. Karmalkar, *J. Appl. Phys.* **99**, 093701 (2006).

10. J.W.P. Hsu, M.J. Manfra, R.J. Molnar, B. Heying, and J.S. Speck, *Appl. Phys. Lett.* **81**, 79 (2002).
11. J.H. Werner and H.H. Guttler, *J. Appl. Phys.* **69**, 1522 (1991).
12. J.P. Sullivan, R.T. Tung, M.R. Pinto, and W.R. Graham, *J. Appl. Phys.* **70**, 7403 (1991).
13. R.T. Tung, *Phys. Rev. B* **45**, 13509 (1992).
14. K. Sarpatwari, S.E. Mohny, and O.O. Awadelkarim, *J. Appl. Phys.* **109**, 014510 (2011).
15. M. Biber, O. Gullu, S. Forment, R.L. Van Meirhaeghe, and A. Turut, *Semicond. Sci. Technol.* **21**, 1 (2006).
16. I. Tascioglu, U. Aydemir, and S. Altindal, *J. Appl. Phys.* **108**, 064506 (2010).
17. N. Yildirim, K. Ejderha, and A. Turut, *J. Appl. Phys.* **108**, 114506 (2010).
18. M. Mamor, *J. Phys. Condens. Matter* **21**, 335802 (2009).
19. F. Iucolano, F. Roccaforte, F. Giannazzo, and V. Raineri, *J. Appl. Phys.* **102**, 113701 (2007).
20. F. Iucolano, F. Roccaforte, F. Giannazzo, and V. Raineri, *Appl. Phys. Lett.* **90**, 092119 (2007).
21. S.K. Cheung and N.W. Cheung, *Appl. Phys. Lett.* **49**, 85 (1986).
22. D. Gromov and V. Pugachevich, *Appl. Phys. A* **59**, 331 (1994).
23. D.K. Schroder, *Semiconductor Material and Device Characterization* (Wiley, Hoboken, NJ, 2006).
24. S. Zhu, R.L. Van Meirhaeghe, C. Detavernier, G.-P. Ru, B.-Z. Li, and F. Cardon, *Solid State Commun.* **112**, 611 (1999).
25. M.O. Aboelfotoh, *J. Appl. Phys.* **66**, 262 (1989).
26. V.G. Bozhkov and A.V. Shmargunov, *J. Appl. Phys.* **109**, 113718 (2011).
27. T. Markvart and L. Castaner, *Practical Handbook of Photovoltaics. Fundamentals and Application* (Elsevier, New York, 2003).
28. R.F. Schmitsdorf, T.U. Kampen, and W. Monch, *J. Vac. Sci. Technol. B* **15**, 1221 (1997).
29. T.P. Chen, T.C. Lee, C.C. Ling, C.D. Beling, and S. Fung, *Solid State Electron.* **36**, 949 (1993).
30. Y.-L. Jiang, G.-P. Rua, F. Lu, X.-P. Qu, B.-Z. Li, and S. Yang, *J. Appl. Phys.* **93**, 866 (2003).
31. J.M. Andrews and M.P. Lepselter, *Solid State Electron.* **13**, 1011 (1970).

Received 13.02.12.

Translated from Ukrainian by O.I. Voitenko

О.Я. Олих

ОСОБЛИВОСТІ ПЕРЕНЕСЕННЯ ЗАРЯДУ  
В СТРУКТУРАХ Mo/*n*-Si З БАР'ЄРОМ ШОТКИ

## Резюме

У роботі експериментально досліджено прямі та зворотні вольт-амперні характеристики структур Mo/*n*-Si з бар'єром Шотки в діапазоні температур 130–330 К. Виявлено, що при підвищенні температури має місце збільшення висоти бар'єра Шотки та зменшення фактора неідеальності. Проведено аналіз отриманих результатів у рамках моделі неоднорідного контакту. Визначено середнє значення та стандартне відхилення висоти бар'єра Шотки: 0,872 В та 0,099 В при  $T = 130\text{--}220$  К і 0,656 В та 0,036 В при  $T = 230\text{--}330$  К відповідно. Показано, що при зворотному зміщенні основними процесами перенесення заряду є термоелектронна емісія через неоднорідний бар'єр та тунелювання.